Pharmaceutical Sciences and Drug Design
ISSN: 3062-4428
2025, Volume 5, Issue 2, Page No: 261-271

Available online at: www.galaxypub.co/page/journals

Galaxy Publication

Galaxy Publication

Polypharmacological Profiling of 3-[5-(1H-Indol-3-ylmethylene)-4-oxo-2-thioxothiazolidin-3-yl]-propionic Acid (Les-6614): Antimicrobial, Anti-Inflammatory, and Receptor-Binding Insights

Sanjay Kulkarni[1], Meenal Joshi[1]*, Rohan Patil[2], Aniket Deshmukh[2]

[1]Department of Pharmaceutical Sciences and Drug Design, Faculty of Pharmacy, Savitribai Phule Pune University, Pune, India.
[2]Department of Drug Discovery Systems, Faculty of Pharmaceutical Sciences, IIT Bombay, Mumbai, India.

***E-mail** ✉ meenal.joshi@gmail.com

Received: 14 September 2026; **Revised:** 02 December 2026; **Accepted:** 05 December 2026

ABSTRACT

Identifying new biological activities in already-discovered hit compounds is a fundamental challenge in modern medicinal chemistry. Our investigation examined the previously studied 3-[5-(1H-indol-3-ylmethylene)-4-oxo-2-thioxothiazolidin-3-yl]-propionic acid (Les-6614) for antimicrobial, antifungal, anti-allergic, and antitumor activities. Cytotoxicity profiling, molecular docking, and SwissADME online target prediction were also carried out. The findings revealed that Les-6614 possesses modest antimicrobial and antitumor capabilities. By contrast, the test compound produced a 33–86% reduction in IgE levels in sensitized guinea pigs and suppressed IgA, IgM, IL-2, and TNF-α, suggesting anti-inflammatory and anti-allergic potential. Target projections for Les-6614, generated by the SwissADME web tool, indicate possible affinities for lysosomal protective protein, Thromboxane-A synthase, and PPARγ. Docking simulations corroborated that the studied 2-thioxo-4-thiazolidinone derivative binds favorably to both LLP and TXAS, yielding stable protein–ligand assemblies. Beyond this, Les-6614 emerges as a candidate PPARγ modulator, a role relevant to the pathogenesis of allergic conditions, malignancies, and cardiovascular disorders.

Keywords: 2-thioxo-4-thiazolidinones, Antimicrobial activity, Guinea pigs, Inflammation, Toxicity, Molecular docking

How to Cite This Article: Kulkarni S, Joshi M, Patil R, Deshmukh A, Polypharmacological Profiling of 3-[5-(1H-Indol-3-ylmethylene)-4-oxo-2-thioxothiazolidin-3-yl]-propionic Acid (Les-6614): Antimicrobial, Anti-Inflammatory, and Receptor-Binding Insights. Pharm Sci Drug Des. 2025;5(2):261-71. https://doi.org/10.51847/Kf6duOlvTY

Introduction

A viable path in drug discovery involves selecting an active molecule as a polypharmacological agent capable of acting on multiple targets, built on the notion of "single agent on multiple targets for single/multiple disease/es" [1]. A molecule's failure to produce a marked effect against one particular target does not automatically render it unpromising, especially as the roster of newly studied targets expands annually. At times, a considerable gap between the molecule's strong effect and its direct target engagement can suggest minimal toxicity along with the feasibility of extended-duration action.

In the pursuit of novel hit compounds and drug candidates, standardizing the screening workflow remains a persistent difficulty [2]. Typically, a narrow panel of targets is assessed, which streamlines selection of the most potent molecule but excludes smaller, specialized targets. On the flip side, engaging a broad array of biological targets in the screen substantially increases costs, often failing to boost overall efficiency. Achieving the "golden mean" in optimizing the screening of bioactive molecules remains a pressing concern for both major pharmaceutical enterprises and small academic drug-discovery teams [3].

The present manuscript showcases a single selected molecule assessed via multiple methodologies against diverse targets, acting as a representative case of a weakly active derivative lacking a single dominant pharmacological

effect while retaining notable promise for future investigation. In the work described here, we explored the previously synthesized 2-thioxo-4-thiazolidinone (rhodanine) derivative, Les-6614 **(Figure 1)**, as a prospective agent with antimicrobial/antifungal/anti-allergic/anti-inflammatory/antitumor properties.

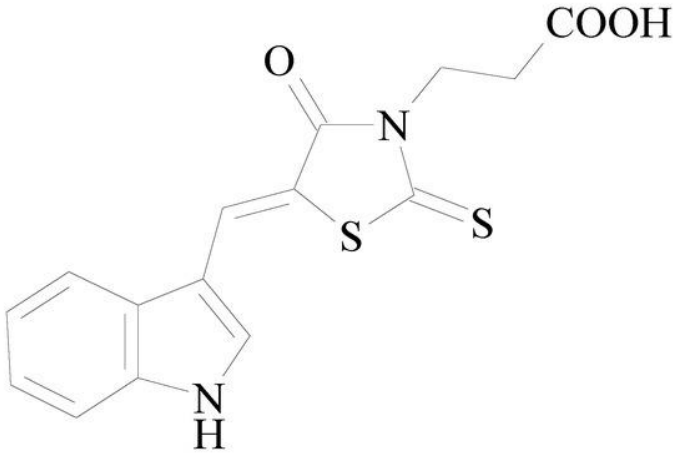

Figure 1. Structure of 3-[5-(1H-indol-3-ylmethylene)-4-oxo-2-thioxo-thiazolidin-3-yl]-propionic acid (Les-6614).

Our prior publications covered the preparation of 5-indolylmethylene-3-substituted rhodanines via Knoevenagel condensation of rhodanine-3-propanoic/ethanesulfonic acids and their corresponding esters with indole-3/6-carbaldehydes [4, 5]. Out of the entire collection of synthesized products, 3-[5-(1H-indol-3-ylmethylene)-4-oxo-2-thioxothiazolidin-3-yl]-propionic acid (Les-6614) displayed the most pronounced activity. Earlier, we established that this specific compound exhibits low toxicity, low-to-moderate antifungal effects, and immunomodulatory properties (elevated quantitative counts of lymphocytes and monocytes with preservation of neutrophilic leukocyte levels, heightened absorptive capacity of phagocytes paralleled by a concurrent drop in phagocytosis completion rates, and an increased proportion of CD3 and CD8 T-lymphocytes contrasted with a diminished relative abundance of natural killer cells and CD22 B-lymphocytes).

Materials and Methods

Antimicrobial activity

The derivative Les-6614 was examined in vitro for its capacity to inhibit bacterial and fungal growth using agar diffusion and the resazurin-based microdilution assay (RBMA) [6, 7]. An agar well of 5.5 mm in diameter received 100 µL (1 mg/mL) of the tested substance. A micrometer, precise to within 0.1 mm, served to quantify the zone of growth suppression. Controls consisted of dimethyl sulfoxide (DMSO) (Sigma-Aldrich, St. Louis, MO, USA), vancomycin discs (Thermo Fisher Scientific Inc., Waltham, MA, USA), ciprofloxacin discs (Thermo Fisher Scientific Inc., Waltham, MA, USA), and clotrimazole discs (Mast Group Ltd., Liverpool, UK). Neat DMSO served as the vehicle due to the limited miscibility of the analog in dilute DMSO. Mueller-Hinton agar (Sigma-Aldrich, St. Louis, MO, USA) and Sabouraud agar (Sigma-Aldrich, St. Louis, MO, USA) were used for bacteria and fungi, respectively, with bacterial plates incubated at 37 °C for 24 h and fungal plates at 25 °C for 24–48 h. In the RBMA format, each well of a 96-well plate received 50 µL of growth medium (Mueller-Hinton or glucose broth), 50 mL of the microorganism suspension adjusted to McFarland 1.0–1.5, and 100 µL of the compound, after which 15 µL of 0.02% resazurin was dispensed into every well. The assay panel included 23 reference and clinical bacterial and fungal isolates **(Table 1)**, whose identities had been confirmed previously by MALDI-TOF (Bruker, Bremen, Germany) and 16S rRNA gene sequencing. Every clinical isolate was multidrug-resistant or extensively drug-resistant and displayed a unique antibiotic resistance fingerprint. These pathogens were recovered from patients diagnosed with healthcare-associated infections (respiratory, bloodstream, and urinary tract) at regional hospitals. All experiments were performed three times.

Table 1. In vitro antimicrobial activity of Les-6614 (zone of growth inhibition at conc. 1 mg/mL after 24–48 h and MIC value μM).

N	Microorganism Type	Species (Bacteria/Fungi)	Clotrimazole	Ciprofloxacin	Vancomycin	DMSO	Zone of growth inhibition (mm ± SE) – Les-6614
1	Gram-negative bacteria (reference)	*Pseudomonas aeruginosa* ATCC 10145	–	35.0 ± 0.3	–	7.0 ± 0.3	7.0 ± 0.3
2	Gram-negative bacteria (reference)	*Raoultella terrigena* ATCC 33257	–	42.0 ± 0.5	–	6.5 ± 0.25	6.5 ± 0.25
3	Gram-negative bacteria (reference)	*Raoultella ornithinolytica* DSM 7464	–	40.0 ± 0.5	–	7.0 ± 0.3	7.0 ± 0.3
4	Gram-negative bacteria (reference)	*Escherichia coli* ATCC 25922	–	28.0 ± 0.5	–	n/a	n/a
5	Gram-negative bacteria (clinical)	*Klebsiella pneumoniae* 189	–	20.0 ± 0.2	–	n/a	n/a
6	Gram-negative bacteria (clinical)	*Aeromonas hydrophila* N196	–	27.0 ± 0.4	–	n/a	8.0 ± 0.25
7	Gram-negative bacteria (clinical)	*Escherichia coli* N168	–	15.3 ± 0.2	–	n/a	n/a
8	Gram-negative bacteria (clinical)	*Morganella morganii* N55	–	21.0 ± 0.4	–	7.0 ± 0.3	7.0 ± 0.3
9	Gram-negative bacteria (clinical)	*Kocuria marina* N133	–	27.5 ± 0.5	–	7.0 ± 0.3	7.0 ± 0.3
10	Gram-positive bacteria (reference)	*Streptococcus agalactiae* ATCC 13813	–	–	32.0 ± 0.5	n/a	8.8 ± 0.25
11	Gram-positive bacteria (reference)	*Staphylococcus aureus* ATCC 25923	–	35.0 ± 0.5	32.0 ± 0.5	n/a	9.4 ± 0.4
12	Gram-positive bacteria (reference)	*Staphylococcus epidermidis* ATCC 12228	–	52.5 ± 0.8	25.0 ± 0.5	12.0 ± 0.5	9.5 ± 0.5
13	Gram-positive bacteria (reference)	*Bacillus subtilis* ATCC 6633	–	–	27.0 ± 0.5	7.4 ± 0.2	9.4 ± 0.2
14	Gram-positive bacteria (clinical)	*Staphylococcus aureus* N23	–	9.0 ± 0.2	11.4 ± 0.3	n/a	8.2 ± 0.4
15	Gram-positive bacteria (clinical)	*Enterococcus faecalis* N26	–	13.3 ± 0.5	11.1 ± 0.3	n/a	n/a
16	Gram-positive bacteria (clinical)	*Enterococcus faecalis* N191	–	13.4 ± 0.5	11.0 ± 0.4	n/a	n/a
17	Fungi (reference)	*Candida albicans* ATCC 885-653	18.0 ± 0.5	–	–	n/a	9.0 ± 0.4
18	Fungi (clinical)	*Candida albicans* N67	11.0 ± 0.3 / MIC 2.9 μM	–	–	n/a	9.0 ± 0.3 / MIC 3003 μM
19	Fungi (clinical)	*Candida guilliermondii* N83	11.0 ± 0.3	–	–	n/a	n/a
20	Fungi (clinical)	*Candida utilis* N127	11.0 ± 0.3	–	–	n/a	n/a
21	Fungi (clinical)	*Candida kefyr* N92	11.0 ± 0.3	–	–	n/a	n/a
22	Fungi (clinical)	*Candida lusitaniae* N89	11.0 ± 0.3	–	–	n/a	7.0 ± 0.3
23	Fungi (clinical)	*Saccharomyces cerevisiae* N62	8.0 ± 0.2	–	–	n/a	7.0 ± 0.4

Vancomycin 30 μg (inhibition zone 17–21 mm for *S. aureus*); ciprofloxacin 5 μg (inhibition zone 25–33 mm for *P. aeruginosa*, 22–30 mm for *S. aureus*, 30–40 mm for *E. coli*); clotrimazole 10 μg (inhibition zone 12–17 mm for *Candida* spp.; diameter of well 5.5 mm; n/a no activity.

Cytotoxicity and antitumor effect in vitro cell lines

Cell lines HCT-116 wt, MCF-7, KB3-1, K562, J774.2, NIH 3T3, and HaCaT were generously donated by a Collection housed at the Institute of Molecular Biology and Genetics, National Academy of Sciences of Ukraine

(Kyiv, Ukraine). The p53-null HCT-116 p53(-/-) colon carcinoma variant was gifted by the Collection of the Institute for Cancer Research, Vienna Medical University (Vienna, Austria). All cultures were maintained either in Dulbecco's Modified Eagle Medium (DMEM, Biowest, Nuaillé, France) or RPMI-1640 (Biowest, France), each supplemented with 10% fetal bovine serum (FBS, Biowest, Nuaillé, France), following ATCC specifications, and kept in a humidified 5% CO2 atmosphere at 37 °C.

MTT assay for measuring cell viability

Cytotoxic activity was gauged through the MTT (3-[4,5-dimethylthiazol-2-yl]-2,5-diphenyl tetrazolium bromide) reduction assay (Sigma-Aldrich, St. Louis, MO, USA). Into each well of 96-well plates, either 4000 adherent cells or 15,000 suspension cells were placed in 100 µL of DMEM or RPMI-1640 containing 10% heat-inactivated FBS, and co-incubated for 72 h at 37 °C under 5% CO_2 with the compound applied at 1, 10, and 100 µM final concentrations. Afterward, the culture supernatant was discarded, and MTT solution (5 mg/mL) was added for an additional 4 h. Formazan precipitates were solubilized in dimethyl sulfoxide. Optical densities were collected with an Absorbance Reader BioTek ELx800 (BioTek Instruments Inc., Winooski, VT, USA). Nonlinear regression in GraphPad Prism 8 v. 8.0.1 (GraphPad Software, San Diego, CA, USA) yielded the half maximal inhibitory concentration (IC50). Data were handled within GraphPad Prism 8 v. 8.0.1 and presented as mean (M) ± standard deviation (SD) from three independent replicates [8].

Animals and immunological (ELISA) studies

The allergenic potential of the compound was explored following standard protocols [9, 10]. Sensitization was induced by injecting 200 µg of the derivative intradermally into the skin covering the outer ear, using 0.02 mL of carrier (saline for the pure control cohort and 20% ethanol in water). Control subjects received 0.02 mL of the carrier only. After a 10-day pause, 20 supplementary epicutaneous applications were administered to a shaved patch on the lateral body surface. The sensitization grade was subsequently evaluated via intradermal challenge tests employing 1:10 and 1:100 dilutions [11-13]. Immunological readouts were obtained with erythrocyte-based diagnostic kits (TOV NVL "Granum", Kharkiv, Ukraine) and ELISA plates specific for guinea pig interleukin 6, guinea pig IgG, guinea pig IgA, guinea pig IgM, and guinea pig tumor necrosis factor alpha, each kit accommodating 48 determinations (MyBioSource, Inc., San Diego, CA, USA).

Molecular and pharmacokinetic properties

Physicochemical descriptors and ADMET (absorption, distribution, metabolism, excretion, toxicity) attributes of (Z)-3-(5-((1H-indol-3-yl)methylene)-4-oxo-2-thioxothiazolidin-3-yl)propanoic acid were forecast using the SwissADME web tool operated by the Swiss Institute of Bioinformatics [http://www.swissadme.ch/index.php accessed on 20 November 2022].

Molecular docking

The structure was sketched in ChemDraw v.18.0.0.231 (PerkinElmer, Waltham, MA, USA) and its energy minimized via Avogadro (open-source, freely distributed software) applying the MMFF94 force field within a molecular mechanics framework [14]; protonation states were set to mimic pH 7.4.

The chosen protein targets comprised lysosomal protective protein LPP (PDB entry 4CIA), PPARγ (PDB entry 5Y2O), vascular endothelial growth factor receptor 2 VEGFR2 (PDB entry 4AGD), and thromboxane A2 synthase (TXAS). VEGFR2 was selected because Les-6614 shares a scaffold with sunitinib, a known multi-kinase inhibitor. As no experimentally resolved structure was available for thromboxane A2 synthase, a homology model was built through the SwissADME server (https://swissmodel.expasy.org/ accessed on 20 November 2022). The model quality metrics GMQE and QMEANDisCo reached 0.67 and 0.70 ± 0.05, respectively, supporting its reliability. Co-crystallized ligands of LPP, PPARγ, and VEGFR2 served as reference comparators, whereas dazoxiben acted as the reference inhibitor for thromboxane A2 synthase [15]. Grid dimensions for docking were set to 60 × 60 × 60 Å, with a grid-point spacing of 0.375 Å. All docking runs utilized AutoDock4 coupled with the Lamarckian genetic algorithm (LGA) [16]. The number of GA runs was increased to 50, and the population size was set to 300, while other parameters remained at factory defaults. The resulting RMSD values were consistently ≤2 Å, confirming the docking workflow's ability to faithfully reproduce the experimentally observed binding poses and its suitability for investigating alternate binders. Non-covalent interactions—hydrogen bonds

together with other nonbonded contacts—between the derivative and the proteins were analyzed and depicted using Biovia Discovery Studio Visualizer v. 21.1.0.20298 (Dassault Systèmes, Vélizy-Villacoublay, France).

Statistical analysis

Statistical computations were conducted in Microsoft Excel. All values are quoted as the arithmetic mean (M) alongside standard deviation (m). Comparisons were made using Student's t-test, with $P < 0.05$ adopted as the cutoff for significance.

Results and Discussion

Antimicrobial activity

Encouraged by earlier observations of antimicrobial effects linked to 3-[5-(1H-indol-3-ylmethylene)-4-oxo-2-thioxothiazolidin-3-yl]-propionic acid and rhodanine-based structures as a chemical class [17, 18], we proceeded to screen supplementary microbial isolates. The substance demonstrated only marginal antibacterial potency toward a limited set of Gram-positive and Gram-negative organisms. Yet, it did exert a weak-to-moderate inhibitory influence on yeast-like fungi (MIC value of 3003 μM, corresponding to 25 μg/mL, when assayed against Candida albicans 67) **(Table 1).**

Cytotoxicity and antitumor effect in vitro

Les-6614 was likewise assessed for its growth-suppressive capacity in several cancer-derived cell lines, namely colorectal (HCT-116, HCT-116 p53-/-), mammary (MCF-7), leukemic (K562), and cervical (KB3-1). Virtually no reduction in cell survival was detected across any of the malignant lines under study. The K562 line proved the most susceptible, yielding an IC50 figure of 83.20 μM, whereas IC50 determinations for the rest of the panel lay above the 100 μM mark **(Table 2).**

Table 2. IC50 value of Les-6614 for a panel of human and animal cell lines (MTT test, 72 h, m ± SD, μM).

Comp./Cell Line	HaCaT	NIH 3T3	J774.2	K562	KB3-1	MCF-7	HCT-116 p53-/-	HCT-116
Les-6614	>100	>100	98.00 ± 2.30	83.20 ± 2.25	>100	>100	>100	>100
Doxorubicin	>10	1.56 ± 0.22	1.20 ± 0.53	1.34 ± 0.4	1.20 ± 1.38	1.53 ± 1.40	1.36 ± 0.91	0.57 ± 1.22

Toxic effects were also measured on non-malignant murine J774.2 macrophages, NIH 3T3 embryonic fibroblasts of mouse origin, and HaCaT human keratinocytes. Les-6614 exerted its greatest effect on the J774.2 macrophage population, with an IC50 of 98 μM **(Table 2)**. By all indications, the molecule lacks meaningful cancer-selective cytotoxicity. When set alongside doxorubicin—a classic anticancer drug employed here as a reference compound that returned IC50 values spanning 0.57 to >10 μM across the same panel—the test article barely perturbed the viability of either tumorigenic or near-normal human and rodent cell types.

Immunological (ELISA) studies

Examination of humoral and cytokine markers in the sera of treated animals revealed a significant 21.4% reduction in IgA titers ($P < 0.05$), concomitant with a significant 21.2% increase in IgG concentrations. All remaining immunoglobulin classes **(Table 3)** declined, and IgE showed the most precipitous decrease, amounting to 86.8%.

Table 3. Quantitative indicators of the levels of immunoglobulins and interleukins in the serum of laboratory animals under the influence of the tested Les-6614.

Indicator	P	Change %	75 Per *	25 Per *	Les-6614	75 Per *	25 Per *	Control
Ig E, ng/mL		−86.82	40.80	< 2.3	22.9	183.80	21.60	173.7
Ig E &, ng/mL		−33.93	144.1	103.4	161.6	302.7	200.4	244.6
Ig A, g/L	< 0.05	−35.29			1.1 ± 0.1			1.6 ± 0.2
IgM, g/L	> 0.05	−12.73			0.48 ± 0.02			0.55 ± 0.04
Ig G, g/L	< 0.05	21.18			10.3 ± 0.2			8.5 ± 0.3

IL-2, pg/mL	−33.54	106	7.1	76.9	144	100.7	115.7
IL-6, pg/mL	7.19	296.8	249.5	276.11	285.2	240.8	257.6
TNF-α, pg/mL	−41.12	27.6	21.1	26.2	58.2	28.6	44.5

The 25/75 percentile represents incorrect distribution; the correct distribution is represented by Student's t-test (P), and using a kit from another distributor.

Analysis of the cytokine component of the profile indicated a slight decrease in IL-2 and TNF-α, two mediators classically associated with Th1-driven cellular immune pathways. A small increase in IL-6 was instead observed, a cytokine more closely involved in tuning the overall immune response.

Molecular and pharmacokinetic properties

Computational ADME profiling executed via the SwissADME server indicated that Les-6614 falls within the boundaries of Lipinski's rule of five, is predicted to undergo efficient uptake from the gastrointestinal tract, and lacks the physicochemical features required for central nervous system penetration. The computed log Po/w descriptor implied adequate membrane transit compatible with oral dosing. The P- glycoprotein classifier did not flag the compound, suggesting that active efflux is unlikely to dictate its clearance. A negative value for skin permeation indicates poor transdermal permeation.

In contrast, the same SwissADME analysis predicted a potential metabolic interaction with a subset of cytochrome P450 (CYP) enzymes, notably CYP1A2, CYP2C19, CYP2C9, and CYP3A4. When viewed in their entirety, the in silico descriptors position Les-6614 as a drug-like entity meriting continued characterization **(Table 4)**.

Table 4. Physicochemical and pharmacokinetic properties of the studied Les-6614.

No.	Category	Descriptor	Value
1	Physicochemical properties	Molecular weight	332.40
2	Physicochemical properties	Number of heavy atoms	22
3	Physicochemical properties	Number of aromatic heavy atoms	9
4	Physicochemical properties	Number of rotatable bonds	4
5	Physicochemical properties	Hydrogen bond acceptors	3
6	Physicochemical properties	Hydrogen bond donors	2
7	Physicochemical properties	Molar refractivity	94.48
8	Physicochemical properties	Topological polar surface area (TPSA, Å²)	130.79
9	Physicochemical properties	Consensus log P (o/w)	2.29
10	Physicochemical properties	Lipinski rule compliance	Yes
11	Pharmacokinetics	Gastrointestinal absorption	High
12	Pharmacokinetics	Blood–brain barrier permeability	No
13	Pharmacokinetics	P-glycoprotein substrate	No
14	Pharmacokinetics	CYP1A2 inhibition	Yes
15	Pharmacokinetics	CYP2C19 inhibition	Yes
16	Pharmacokinetics	CYP2C9 inhibition	Yes
17	Pharmacokinetics	CYP2D6 inhibition	No
18	Pharmacokinetics	CYP3A4 inhibition	Yes
19	Pharmacokinetics	Skin permeation log Kp (cm/s)	−6.48
20	Pharmacokinetics	Bioavailability score	0.56

As a next step in our virtual screening campaign, we applied similarity searching via the SwissSimilarity interface, which performs multiple two-dimensional comparisons, underpinned by FP2 topological fingerprints, to retrieve close neighbors of drugs or bioactive substances from assembled small-molecule repositories [19]. The scale for these similarity assessments ranges from 0 (wholly unrelated structures) to 1 (indistinguishable entities). A path-based (linear) fingerprint query of the DrugBank catalog returned four entries, with similarity coefficients ranging from 0.511 to 0.580. The identified compounds are recognized to interact with a diverse set of protein targets: the lethal factor produced by Bacillus anthracis (s.s. 0.580), glycylpeptide N-tetradecanoyltransferase 2 (s.s. 0.567), the catalytic gamma isoform of phosphatidylinositol 4,5-bisphosphate 3-kinase (s.s. 0.536), and a serine/threonine protein kinase (s.s. 0.511).

Stimulated by earlier observations, we placed a particular emphasis on uncovering plausible macromolecular interaction partners for (Z)-3-(5-((1H-indol-3-yl)methylene)-4-oxo-2-thioxothiazolidin-3-yl)propanoic acid. The SwissTargetPrediction platform—an internet-based resource that assigns putative protein targets by gauging chemical resemblance between query structures and comprehensively annotated ligand sets [20]—returned lysosomal protective protein (UniprotID: P10619, CHEMBL ID: 6115), thromboxane-A synthase (UniprotID: P24557, CHEMBL ID: 1835), and peroxisome proliferator-activated receptor gamma (UniprotID: P37231, CHEMBL ID: 235) as the three foremost predictions ranked by similarity to the test compound.

Molecular docking

A powerful tactic for identifying promising leads from an array of synthesized derivatives is to perform docking studies, which illuminate the path toward optimal structural alterations that can boost the biological potency of successor compounds. Consequently, in silico docking workflows constitute an invaluable source of data to inform subsequent rounds of structure-guided optimization of previously flagged active molecules.

In the work reported here, molecular docking analyses were performed to map the binding orientations of the test compound when complexed with therapeutically relevant protein receptors. All docking procedures employed AutoDock Tool v. 1.5.6 (Scripps Research, San Diego, CA, USA) to calculate binding free energies, derive inhibition constants, and visualize the predominant geometries of potential ligand–target conjugates.

The docking calculations revealed a pattern of moderate affinity across the entire set of evaluated proteins, reinforcing the proposition that the compound can serve as a starting template for the future development of drug-like compounds with an improved pharmacological profile. A summary of the computational outcomes is provided in **Table 5**.

Table 5. Molecular docking results for Les-6614.

Compound	Target (PDB ID)	Ki (μM, TXAS)	Binding Energy (TXAS)	Ki (μM, VEGFR2)	Binding energy (VEGFR2, 4AGD)	Ki (μM, PPARγ)	Binding energy (PPARγ, 5Y2O)	Ki (μM, LPP)	Binding energy (LPP, 4CIA)
Compound	multi-target	0.225	−9.07	0.121	−9.43	0.60	−8.49	0.62	−8.47
6KZ 1	LPP (4CIA)	–	–	–	–	–	–	0.125	−9.42
Pioglitazone	PPARγ (5Y2O)	–	–	–	–	0.00024	−13.12	–	–
Sunitinib	VEGFR2 (4AGD)	–	–	0.00057	−12.61	–	–	–	–
Dazoxiben	TXAS	0.037	−10.14	–	–	–	–	–	–

1 6KZ—PDBe Ligand Code from PDB structure of 4CIA, reported inhibitor of the cathepsin A.

From these data, the most encouraging trajectories for generating new bioactive candidates rooted in the original chemotype involve pursuing fresh LLP and TXAS inhibitors. The binding energies of the two aforementioned macromolecules are close to those computed for their respective co-crystallized ligands, thereby lending credence to the predictive algorithm hosted by the SwissADME portal. The anticancer signature detected for the molecule may be attributable to its weak engagement with PPARγ and VEGFR2; however, the present results do not support definitive mechanistic hypotheses for its antiproliferative effects.

This manuscript chronicles the characterization of an individual biologically active entity, Les-6614, which lacks a striking effect on any single discrete target. The substance under investigation showed minimal antibacterial and antifungal properties, a subdued in vitro cytotoxic effect against tumor cells, and was concurrently largely innocuous.

Lysosomal protective protein (UniprotID: P10619), whose catalytic domain is embodied by cathepsin A, represents one of the computationally nominated targets. Cathepsin A functions as a pivotal overseer of galactoside processing and has been correlated with aggressive disease trajectories and unfavorable prognoses in ductal carcinoma in situ of the breast, potentially doubling as a surrogate indicator for the coexistence of stromal invasion within this tumor type [21, 22]. Members of this protein family, such as the entry designated CHEMBL

ID: 6115, lack PubChem Compound Identifiers but can be easily located by their Uniprot ID [23]. In recent years, CatA has attracted attention as a druggable target for curbing cardiac hypertrophy, given its role in degrading endothelin-1, a molecule that simultaneously promotes vasoconstriction and inflammation [24].

Thromboxane A synthase (Uniprot ID: P24557, CHEMBL ID: 1835) is another target closely linked to cardiovascular conditions. This enzyme operates in concert with the thromboxane prostanoid receptor to exert its physiological effects via a G protein-coupled signaling mechanism, ultimately driving platelet activation, aggregation, and smooth muscle contraction. Pharmacological interference with thromboxane A synthase by the test compound might therefore afford a measure of cardiovascular protection by dampening platelet clumping [25, 26].

Peroxisome proliferator-activated receptor gamma (PPARγ) (UniprotID: P37231, CHEMBL ID: 235) is firmly established as a molecular target relevant to diabetes mellitus; beyond metabolic regulation, PPARγ presides over a diverse array of cell types that participate in the allergen-driven inflammatory cascade, encompassing T helper lymphocytes, airway epithelial cells, and circuits linked to breast tumor development [27-30]. A recent comprehensive survey has identified a potentially robust link between PPARγ and the development of allergic pathologies such as asthma and atopic dermatitis [31], thereby positioning PPARγ modulators as candidate anti-allergy therapeutics. This framework resonates well with the data gathered from our guinea pig model. Administration of the compound led to reductions in IgE of 33–86%, curbed IgA and IgM levels, and diminished IL-2 and TNF-α production, collectively indicating an anti-inflammatory and anti-allergic profile. The precise contribution of PPARγ to the etiopathology of allergic diseases, as well as the intersection of allergy and oncogenesis, remains to be further elucidated.

Inspection of the docking-derived pose suggests that Les-6614 is capable of making contact with the Ser150 side chain belonging to the LLP catalytic triad (completed by Asp372 and His429 [32]) through an oxygen atom projecting from the rhodanine scaffold **(Figure 2)**. Additionally, the carboxyl group engages in a charge-reinforced interaction with His429—the side chain of Tyr247 anchors the ligand via Pi–sulfur and Pi–Pi nonbonded interactions. Meanwhile, Pro301, Cys60, and Cys334 surround the indole and 1,3-thiazole moieties via Pi–Alkyl hydrophobic interactions.

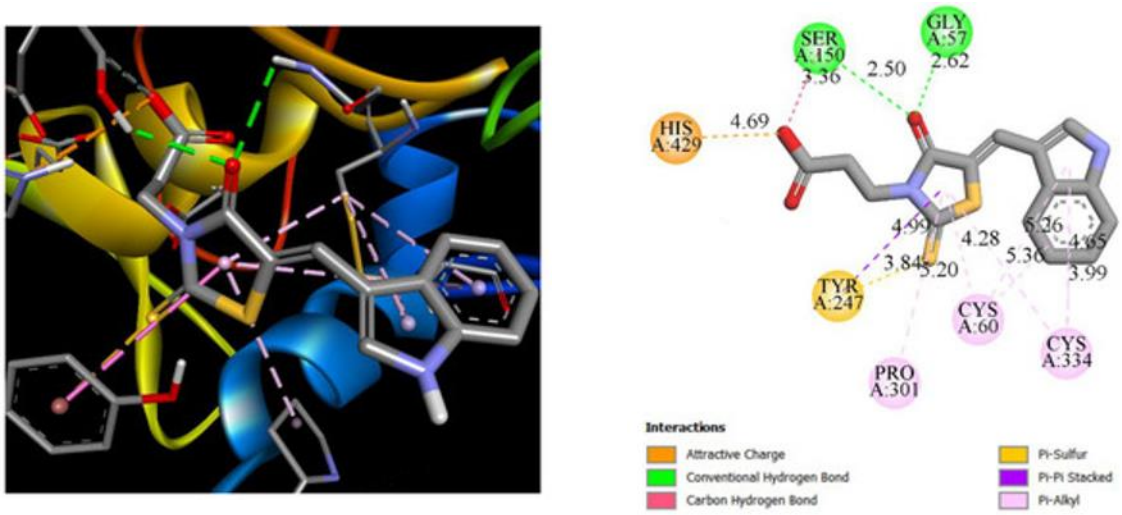

a) b)

Figure 2. The predicted binding mode for the studied Les-6614 with the LLP (PDB 4CIA).

The molecule appears to anchor within the LLP enzyme via a pair of hydrogen bonds, one to Trp132 (2.05 Å) and another to Cys479 (3.69 Å) **(Figure 3)**. Beyond these polar contacts, both the rhodanine and indole scaffolds are stabilized by an array of hydrophobic forces distributed throughout the binding pocket, supplied by lipophilic side chains (encompassing Pi–Sigma, Pi–Sulfur, Pi–Pi T-shaped, and Pi–Alkyl interactions). Three arginine residues establish attractive electrostatic contacts, with a salt bridge involving the carboxyl moiety. Notably, Les-6614 fails to engage the Arg374 side chain—a residue deemed critical for inhibition—setting it apart from previously characterized competitive inhibitors such as dazoxiben and ozagrel [33].

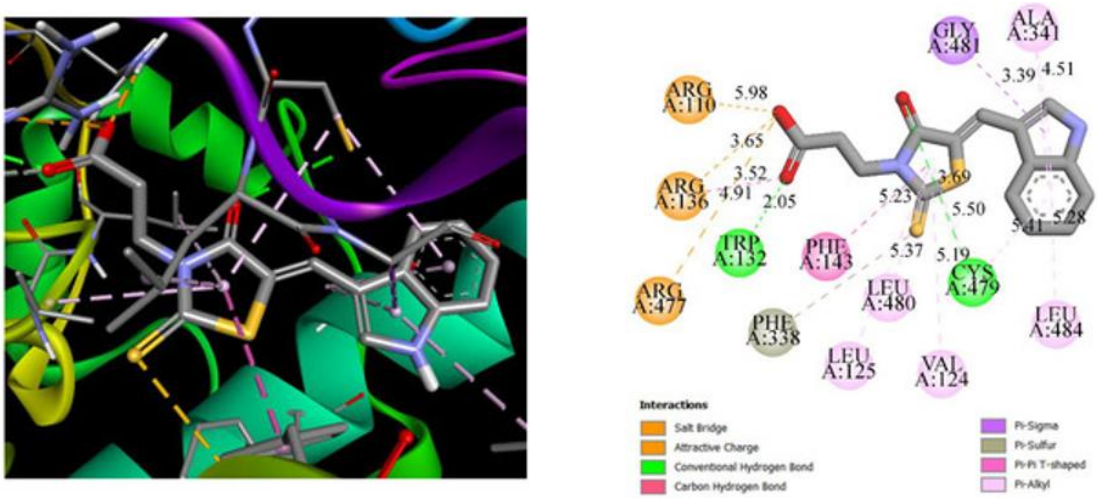

a) b)

Figure 3. The predicted binding mode for Les-6614 with the homology model of the TXAS.

It should be underscored that the docking simulations attribute to the test compound a prospective affinity toward LLP and TXAS, a finding that does not neatly mirror the target predictions generated earlier by the SwissADME platform. This divergence becomes understandable when one examines the molecular architecture of the substance, which belongs to the rhodanine family—a class of compounds widely documented in the literature for their inherent polypharmacology and capacity to engage multiple biological targets concurrently [34-36].

Conclusion

The singled-out molecule Les-6614 was subjected to a range of biological evaluations (antibacterial, antifungal, cytotoxic, antitumor) and further probed using the SwissADME online molecular docking tool. The collective data reveal a diversified activity profile for this rhodanine-based analog, aligning with the concept of a moderately potent "single agent acting on multiple targets for single or multiple diseases." The anti-allergic signature of the compound, potentially traceable to PPARγ modulation, merits particular emphasis. Additionally, docking calculations suggest plausible anticancer properties and the ability to bind the oncologically relevant LLP and TXAS proteins. Taken together, the body of evidence positions 3-[5-(1H-indol-3-ylmethylene)-4-oxo-2-thioxothiazolidin-3-yl]-propionic acid as a well-justified starting scaffold for an innovative class of multi-target therapeutic candidates.

Acknowledgments: The authors thank all the brave defenders of Ukraine who made the finalization of this article possible.

Conflict of Interest: None

Financial Support: The research leading to these results has received funding from the Ministry of Health of Ukraine under the project numbers 0121U100690, 0120U102460, and 0123U100153, and from the National Research Foundation of Ukraine under the project number 2020.02/0035.

Ethics Statement: The permission to conduct experiments on animals and to isolate/work with microorganism cultures was approved under protocol No. 6 of the commission on ethics of scientific research, experimental development, and scientific works of Danylo Halytsky LNMU, Ukraine, dated 25 June 2018.

References

1. Wang Z, Yang B. Polypharmacology. Cham (Switzerland): Springer International Publishing; 2022. ISBN: 978-3-031-04997-2.

2. Anighoro A, Bajorath J, Rastelli G. Polypharmacology: Challenges and opportunities in drug discovery. J Med Chem. 2014;57:7874-87.
3. Hughes J, Rees S, Kalindjian S, Philpott K. Principles of early drug discovery. Br J Pharmacol. 2011;162:1239-49.
4. Konechnyi Y, Hrushka O, Pryzyhley H, Konechna R, Lozynskyi A, Korniychuk O, et al. Cell immunity of laboratory animals under the influence of 5-indolylmethylene rhodanine-3-carboxylic/sulphonic acid derivative. Sci Pharm Sci. 2021;1:76-81.
5. Konechnyi YT, Lozynskyi AV, Horishny VY, Konechna RT, Vynnytska RB, Korniychuk OP, et al. Synthesis of indoline-thiazolidinone hybrids with antibacterial and antifungal activities. Biopolym Cell. 2020;36:381-91.
6. EUCAST. Disk diffusion—manual v10.0. 2022 Jan 1. Available from: https://www.eucast.org/ast_of_bacteria/disk_diffusion_methodology/
7. Balouiri M, Sadiki M, Ibnsouda SK. Methods for in vitro evaluating antimicrobial activity: A review. J Pharm Anal. 2016;6:71-9.
8. Ivasechko I, Yushyn I, Roszczenko P, Senkiv J, Finiuk N, Lesyk D, et al. Development of novel pyridine-thiazole hybrid molecules as potential anticancer agents. Molecules. 2022;27:6219.
9. Suckow MA, Stevens KA, Wilson RP, editors. The Laboratory Rabbit, Guinea Pig, Hamster, and Other Rodents. Cambridge (MA): Academic Press; 2012.
10. Fischbach FT, Dunning MB. A Manual of Laboratory and Diagnostic Tests. Philadelphia (PA): Lippincott Williams & Wilkins; 2009.
11. Alekseyeva O, Duyeva L. Allergy to Industrial Chemical Compounds. Moscow: Medicina; 1978. p. 106-16.
12. Keohane EM, Otto CN, Walenga J. Rodak's Hematology: Clinical Principles and Applications. Amsterdam: Elsevier Health Sciences; 2019.
13. Pagana KD, Pagana T. Mosby's Manual of Diagnostic and Laboratory Tests. Amsterdam: Elsevier Health Sciences; 2017.
14. Halgren TA. Merck molecular force field. I. Basis, form, scope, parameterization, and performance of MMFF94. J Comput Chem. 1996;17:490-519.
15. Schumacher WA, Lucchesi BR. Effect of the thromboxane synthetase inhibitor UK-37,248 (dazoxiben) upon platelet aggregation, coronary artery thrombosis and vascular reactivity. J Pharmacol Exp Ther. 1983;227:790-6.
16. Morris GM, Goodsell DS, Halliday RS, Huey R, Hart WE, Belew RK, et al. Automated docking using a Lamarckian genetic algorithm and an empirical binding free energy function. J Comput Chem. 1998;19:1639-62.
17. Petrou A, Geronikaki A, Kartsev V, Kousaxidis A, Papadimitriou-Tsantarliotou A, Kostic M, et al. N-derivatives of (Z)-methyl 3-(4-oxo-2-thioxothiazolidin-5-ylidene)methyl)-1H-indole-2-carboxylates as antimicrobial agents—in silico and in vitro evaluation. Pharmaceuticals. 2023;16:131.
18. Horishny V, Kartsev V, Geronikaki A, Matiychuk V, Petrou A, Glamoclija J, et al. 5-(1H-Indol-3-ylmethylene)-4-oxo-2-thioxothiazolidin-3-yl)alkancarboxylic acids as antimicrobial agents: Synthesis, biological evaluation, and molecular docking studies. Molecules. 2020;25:1964.
19. Zoete V, Daina A, Bovigny C, Michielin O. SwissSimilarity: A web tool for low to ultra high throughput ligand-based virtual screening. J Chem Inf Model. 2016;56:1399-404.
20. Gfeller D, Grosdidier A, Wirth M, Daina A, Michielin O, Zoete V. SwissTargetPrediction: A web server for target prediction of bioactive small molecules. Nucleic Acids Res. 2014;42:W32-8.
21. Kim JW, Mahiddine F, Kim G. Leptin modulates the metastasis of canine inflammatory mammary adenocarcinoma cells through downregulation of lysosomal protective protein cathepsin A (CTSA). Int J Mol Sci. 2020;21:8963.
22. Toss MS, Miligy IM, Haj-Ahmad R, Gorringe KL, AlKawaz A, Mittal K, et al. The prognostic significance of lysosomal protective protein (cathepsin A) in breast ductal carcinoma in situ. Histopathology. 2019;74:1025-35.
23. Southan C. Caveat usor: Assessing differences between major chemistry databases. ChemMedChem. 2018;13:470-81.
24. Khavrutskii IV, Compton JR, Jurkouich KM, Legler PM. Paired carboxylic acids in enzymes and their role in selective substrate binding, catalysis, and unusually shifted pKa values. Biochemistry. 2019;58:5351-65.

25. Amano H, Nakamura M, Ito Y, Kakutani H, Eshima K, Kitasato H, et al. Thromboxane A synthase enhances blood flow recovery from hindlimb ischemia. J Surg Res. 2016;204:153-63.
26. Mesitskaya DF, Syrkin AL, Aksenova MG, Zhang Y, Zamyatnin AA Jr, Kopylov PY. Thromboxane A synthase: A new target for the treatment of cardiovascular diseases. Cardiovasc Hematol Agents Med Chem. 2019;16:81-7.
27. Vallée A, Lecarpentier Y. Crosstalk between peroxisome proliferator-activated receptor gamma and the canonical WNT/β-catenin pathway in chronic inflammation and oxidative stress during carcinogenesis. Front Immunol. 2018;9:745.
28. Sawant RL, Wadekar JB, Kharat SB, Makasare HS. Targeting PPAR-γ to design and synthesize antidiabetic thiazolidines. EXCLI J. 2018;17:598-607.
29. Sauer S. Ligands for the nuclear peroxisome proliferator-activated receptor gamma. Trends Pharmacol Sci. 2015;36:688-704.
30. Furth PA. Peroxisome proliferator-activated receptor gamma and BRCA1. Endocr Relat Cancer. 2019;26:R73-9.
31. Stark JM, Coquet JM, Tibbitt CA. The role of PPAR-γ in allergic disease. Curr Allergy Asthma Rep. 2021;21:45.
32. Schreuder HA, Liesum A, Kroll K, Böhnisch B, Buning C, Ruf S, et al. Crystal structure of cathepsin A, a novel target for the treatment of cardiovascular diseases. Biochem Biophys Res Commun. 2014;445:451-6.
33. Auch-Schwelk W, Katusic ZS, Vanhoutte PM. Thromboxane A2 receptor antagonists inhibit endothelium-dependent contractions. Hypertension. 1990;15:699-703.
34. Kaminskyy D, Kryshchyshyn A, Lesyk R. Recent developments with rhodanine as a scaffold for drug discovery. Expert Opin Drug Discov. 2017;12:1233-52.
35. Tomašić T, Mašič L. Rhodanine as a privileged scaffold in drug discovery. Curr Med Chem. 2009;16:1596-629.
36. Tomašić T, Peterlin Mašič L. Rhodanine as a scaffold in drug discovery: A critical review of its biological activities and mechanisms of target modulation. Expert Opin Drug Discov. 2012;7:549-60.